Astronomy Letters, Vol. 24, No. 1, 1998, pp. 90–105. Translated from Pis'ma v Astronomicheskii Zhurnal, Vol. 24, Nos. 1–2, 1998, pp. 116–132.

Chemical Composition of the CP Hg–Mn Components of Approximately Equal Mass in the SB2 System 46 Draconis

V. V. Tsymbal[1], O. P. Kotchukhov[1], V. L. Khokhlova[2], and D. L. Lambert[3]

[1] *Simferopol State University, Simferopol, Ukraine*
[2] *Institute of Astronomy, Russian Academy of Sciences, Pyatnitskaya ul. 48, Moscow, 109017 Russia*
[3] *Department of Astronomy, University of Texas, Austin, USA*
Received September 20, 1997

Abstract—We have performed the most complete (to date) atmospheric-abundance analysis of the components of approximately equal mass in the SB2 system 46 Dra using the high-resolution, S/N = > 200 CCD spectra obtained with the echelle spectrograph of the 2.7-m McDonald Observatory telescope. The abundances of 25 elements were determined from lines in the wide spectral range 3800 to 9000 A. The rotation of the components is shown to be synchronized and coaxial with the orbital motion. The chemical anomalies of both components were found to be generally similar: an underabundance of He, C, N, O, and Al; a nearly solar abundance of iron-peak elements; and considerable overabundances of P, Mn, Ga, Sr, Y, Zr, Ba, Pt, Au, and Hg, which increase with increasing atomic number. However, we found significant differences in the abundances of some elements in components A and B, similar to those that were previously detected in the analogous SB2 system AR Aur: an underabundance of Al and Ni in component A with a smaller anomaly or a normal abundance of these two elements in component B. Component A shows a considerably greater overabundance of Ga and considerably smaller overabundances of Sr and Pt than component B does.There are also differences between the systems themselves: in contrast to AR Aur, in which only component A exhibits great overabundances of Y, Ba, and Hg, these elements are equally greatly enhanced in both components of 46 Dra. The most striking difference between components A and B of 46 Dra, which are similar in all physical parameters, is the difference in the isotopic composition of mercury which was first detected by Cowley and Aikman (1975) and confirmed in this study. It is concluded that the abundance difference between the components could arise after the synchronization of the rotation and the arrival of the stars at the main sequence.

1. INTRODUCTION

In recent years, the abundance analyses of the atmospheres of binary stars with a primary or both CP components of Hg–Mn type have markedly intensified. The interest in them is explained by the fact that the parameters (masses, radii) of such systems which are important for determining their evolutionary status can be estimated, and that a comparative analysis of the chemical composition of the components makes it possible to approach to the solution of the problem of the origin of chemical anomalies.

Studies of binary systems with components of equal mass are particularly promising. In this case, one might expect the evolution of stars that were formed out of the same protostellar cloud to differ only slightly. Do the components of such systems have the same chemical composition? The published data on several known stars of this type do not provide an unambiguous answer to this question. In some cases, the most prominent Hg anomaly (an enhanced HgII λ3984 line) appears in the spectrum of only one component; in other cases, it is observed in both components. Subtler differences in the chemical composition of the components have scarcely been studied at all.

We have previously studied the chemical composition of AR Aur, the only known eclipsing system of this type (with the inclination $i = 90°$, which makes it possible to determine all parameters of the system directly from the radial-velocity and light curves) (Khokhlova *et. al.* 1995). This study showed that the abundance of several elements (Al, Ni, Mn, Ba, Sr, Y, Zr, Hg, Pt) differ markedly in both components.

The aim of this paper is a detailed study of another binary system of this type (46 Dra = HR 7049 = HD 173524). In contrast to AR Aur, 46 Dra is not an eclipsing binary, but this is offset by the fact that the narrowness of its spectral lines allows us to perform a detailed analysis of a large number of lines of many elements.

2. PREVIOUS STUDIES OF 46 Dra

The first abundance analysis of 46 Dra was performed by Conti (1970a) who estimated the luminosity ratio of its components by analyzing FeI and FeII lines, $L_A/L_B = 1.60$, and determined the effective temperature, $T_{eff} = 12000$ K; the temperature difference between the components is 250 K. This author also detected overabundance of Sr, Y, Zr, Hg, and Pt in both

1063-7737/98/2401-0090$15.00 © 1998 МАИК Наука/Interperiodica Publishing

components and an overabundance of Mn and Ga only in component A. In his paper, Conti noted a difference in the chemical composition of the components. Aikman (1976) refined the orbital elements of the binary that were previously obtained by Petrie (1935) and Conti (1970b). Adelman and Pyper (1979) determined the effective temperature of 46 Dra from *u–b* photometry, the Balmer jump, and the Paschen continuum. Making no allowance for the binarity, Sadakane *et. al.* (1983) revealed an underabundance of Al using ultraviolet lines. Takada-Hidai *et al.* (1986) detected a Ga overabundance, which, however, was 1–2 dex smaller than that in other studies. Guthrie (1984) noted a considerable enhancement of Mn and Ga in component A compared to the secondary, which, however, exhibits a large overabundance of Pt.

Recently, Adelman *et al.* (1998, below referred to as ARD) have performed the most detailed study of 46 Dra using Reticon spectra with S/N = 200. They determined the luminosity ratio of the components in the wavelength range λ3890–4740 Å from the equivalent widths of FeII lines by assuming that the iron abundances in the two components were equal: $L_A/L_B = 1.7$. ARD used the spectrophotometry of Adelman and Pyper (1979), the Hγ-profile synthesis, and the condition of ionization equilibrium for FeI and FeII lines to ultimately determine the model atmospheres for the components. They assumed the metallicity [Me/H] = +0.2 dex.

ARD confirmed the orbital elements computed by Aikman (1976) but suspected variations in the γ velocity, pointing to the possible existence of a third body in the system with an orbital period of 33.6 ± 2 yr and K = 2.60 ± 0.4 km s^{-1}. However, they detected no lines of this component in their spectra.

The high signal-to-noise ratio allowed ARD to measure weak He I lines in the spectrum of both components and determine the He abundance in them, log (He/H) = –2.00 and –1.78 for components A and B, respectively.

The orbital elements and the parameters of model atmospheres for the components of 46 Dra are given in Table 1.

3. REMARKS ON THE METHOD OF DETERMINING THE ATMOSPHERIC ABUNDANCES IN CP COMPONENTS OF SB2 SYSTEMS

When studying the chemical composition of the atmospheres of CP stars, especially of spectroscopic binaries, we encounter a number of still insufficiently developed methodological issues. This primarily applies to the determination of atmospheric parameters for calculating a model atmosphere of the CP star [see, e.g., Leone and Manfre (1997) or Khokhlova *et. al.* (1997) for a discussion of this problem].

The chemical composition is an atmospheric parameter in itself. A vicious circle arises: in order to determine the chemical composition, we must know the atmospheric structure, but the atmospheric structure depends on the chemical composition. Roughly speaking, the hydrostatic equilibrium and, accordingly, the density distribution in the atmosphere depends on the He/H ratio, while the absorption coefficient, i.e., the temperature distribution depends on the [M/H] ratio.

Table 1

Orbital elements	Conti (1970a, 1970b)	Aikman (1976)	Guthrie (1984)	ARD (1997)
M_A/M_B	1.14	1.175		1.12
L_A/L_B	1.6			1.7
T_{eff} (A), K	12000		11700	11700
T_{eff} (B), K	±125		11400	11100
log$g$ (A)	3.7			4.0
log$g$ (B)	3.9			4.1
[M/H] (A, B)				+0.2
He/H (A)				0.010
He/H (B)				0.017
R_A/R_B				1.23
P, d	9.8109	9.81073 ± 0.00004		
T_0, JD		2440003.22 ± 0.10		2440003.128 ± 0.032
e		0.200 ± 0.015		0.200 ± 0.006
K_A, km s^{-1}		25.1 ± 0.4		26.01 ± 0.17
K_B, km s^{-1}		29.5 ± 0.5		29.12 ± 0.18
γ, km s^{-1}	–29.2	–30.95 ± 0.28		–27.88 ± 0.09

Table 2

JD 2450000+	Phase	V_r (A), km s^{-1}	V_r (B), km s^{-1}	γ, km s^{-1}
206.946483	0.067	−58.23	+1.77	−29.92
207.942717	0.169	−41.57	−16.57	−29.78
208.933089	0.270	−24.92	−36.92	−30.58

Table 3

λ, Å	$\log N_{He}/N_{tot}$ (A)	$\log N_{He}/N_{tot}$ (B)
4026	−2.10	−1.95
4471	−2.03	−1.78
4713	−1.90	−1.70
5875	−1.89	−1.82
6678	−1.90	−1.82
Average	−1.96 ± 0.09	−1.80 ± 0.08

For SB2 systems with CP components, the problem is compounded by the necessity to separate the spectra of the components, i.e., to determine simultaneously the model and the chemical composition of each of them from the overall observed spectrum.

In general, this problem can be solved only by the iteration method. Thus far, no clear-cut algorithm for solving this problem has been worked out. Usually, one intuitively finds a balance of many factors in an effort to obtain consistent atmospheric parameters for fitting the calculated quantities (the Balmer-line profiles, the Paschen continuum energy distribution, etc.) to the observed quantities. As a rule, the spectrophotometric

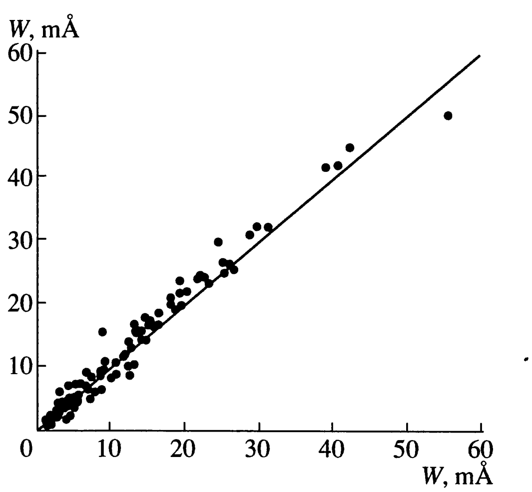

Fig. 1. Comparison of our measured equivalent widths in the spectrum of 46 Dra (x axis) with the ARD data (y axis).

calibrations used to date are based on model atmospheres computed for solar chemical composition.

When determining $\log g$, one does not normally draw or mention a distinction between the spectroscopic $\log g_{eff}$, which is derived from Balmer-line profiles, and the true $\log g$, which is determined by the mass and radius of the star. These values are equal only in the case where the model atmosphere used to determine $\log g_{eff}$ from the Balmer-line profiles is calculated for the actual mean molecular weight (primarily for the actual [He/H]). In order to allow for the He anomalies, a transition from $\log g_{eff}$ to $\log g$ can be made using the formula from Auer *et. al.* (1966).

The method of allowance for metal-abundance anomalies in CP stars has not yet been developed. The question of how the anomalies of individual elements affect the model atmosphere has not been considered. Technically, the problem lies in the necessity to compute the OPDF tables, which allow for blanketing, for the specific abundance anomalies of individual chemical elements. In their model fitting, ARD assumed the metallicity [M/H] = +0.2 with no additional arguments. One might expect that when it will be technically possible to calculate a model atmosphere for the specific abundance of each element, the problem will have so may parameters that it will hardly be possible to actually use it.

Thus, we must recognize that the model-atmosphere parameters cannot claim to have an accuracy that is higher than the scatter of the values given in Table 1. Accordingly, it would be unreasonable to claim a very high accuracy of determining the elemental abundances, at least from temperature-sensitive lines.

Bearing in mind the above discussion and that we did not have any Balmer-line profiles at our disposal at the time of our study, we did not attempt to redetermine the atmospheric parameters of the components of 46 Dra and used in our analysis the parameters obtained in ARD the most detailed and thorough study of all the previous studies.

4. OBSERVATIONS AND REDUCTION OF THE SPECTRA

The spectra of 46 Dra used in this study were obtained in May 1996 with the echelle spectrograph of the 2.7-m McDonald Observatory telescope equipped with a CCD detector (Tull *et. al.* 1995) as part of the observing program of Prof. Lambert with the participation of V.L. Khokhlova. Sixty one spectral orders covered the wavelength range 3600–9800 Å with a spectral resolution of 60000 and S/N ≥ 200.

The initial reduction of the spectra was made at the Department of Stellar Spectra at the University of Texas by V. Woolff with the participation of V.L. Khokhlova using the KPNO–IRAF software package. Further reduction and calculations were performed at the Simferopol University by V.V. Tsymbal and

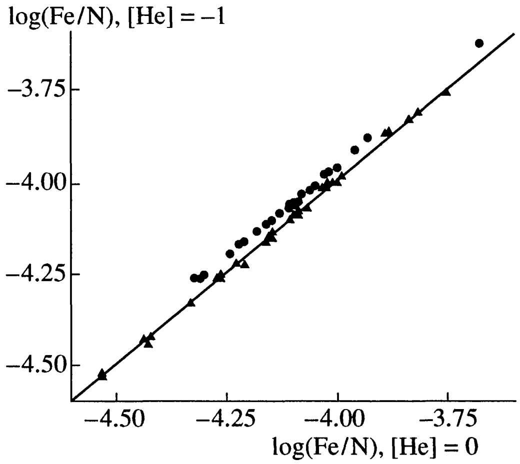

Fig. 2. Comparison of the Fe abundances that were determined from the model atmosphere of 46 Dra computed with an underabundance of He (y axis) with the normal abundance of this element (x axis). The circles and the triangles refer to the FeI and FeII lines, respectively.

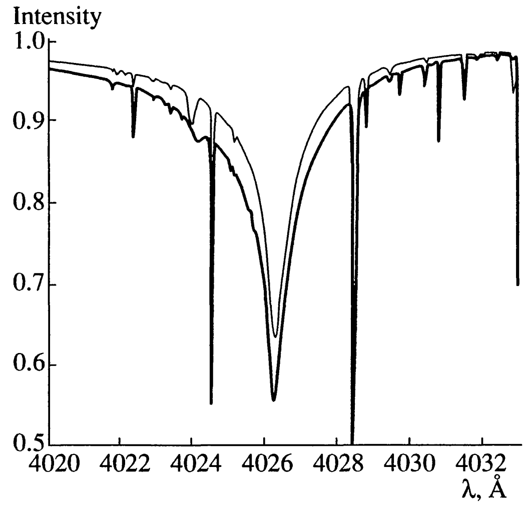

Fig. 3. Profiles of the HeI λ4026 Å line for the model with T_{eff} = 15000 K and log$g$ = 4.0 computed with the Stark broadening from Dmitrievic and Saha-Brechaud (1990) (thin line) and using the unified theory (Barnard *et al.* 1974) (thick line).

O.P. Kotchukhov using the DECH20 (Galazutdinov 1994) and STARSP (Tsymbal 1996) software packages.

Because of the insufficient length of the spectral orders with the Balmer lines and, in some cases, the inaccurate flat fielding during the initial reduction, we failed to use the Balmer lines to refine the model atmospheres for the components of 46 Dra. Table 2 gives the Julian dates of our spectra and the orbital phases that we calculated using the orbital elements of Aikman (1976) and refined by ARD.

Using the orbital elements from Table 1 and the standard equations of celestial mechanics for spectroscopic binaries (Batten 1976), we can easily obtain the quantities

$$M_A \sin^3 i = 0.08482 M_\odot,$$

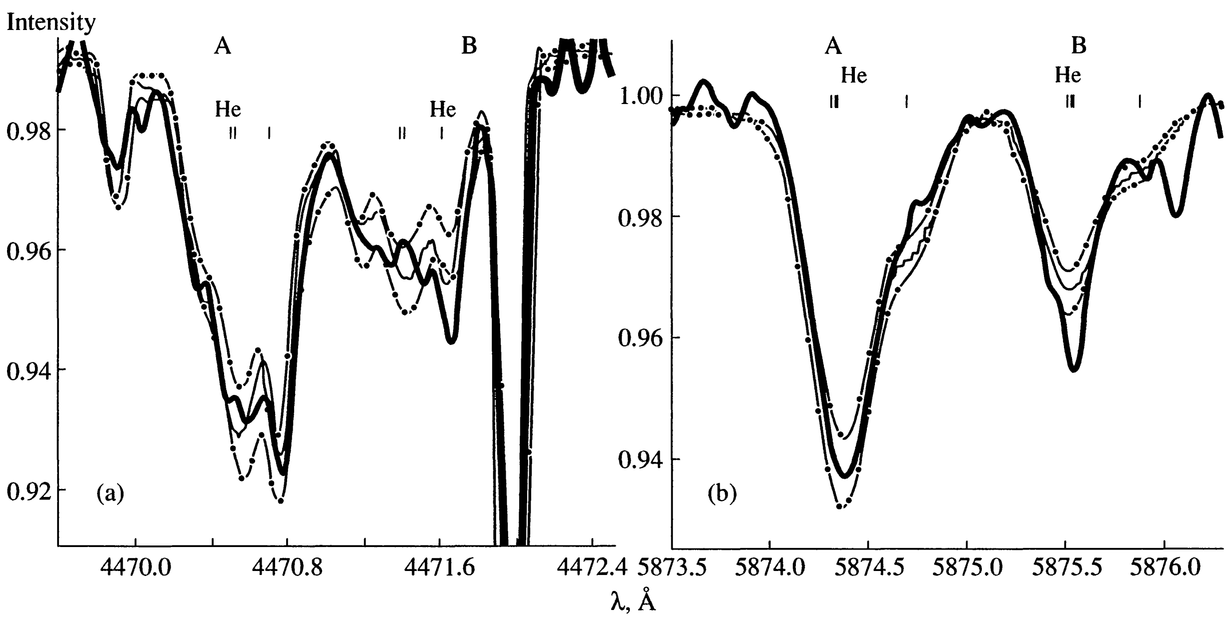

Fig. 4. Spectrum of 46 Dra near the HeI λ4471 Å line (a) and the HeI λ5876 Å line (b): the thick lines are the observed spectrum, the thin lines are the synthetic spectrum, and the dot-dashed lines correspond to a decrease and an increase of the He abundance by 0.1 dex. The positions of the multiplet components are indicated by vertical bars. The wavelength scale in Figs. a and b is a laboratory scale.

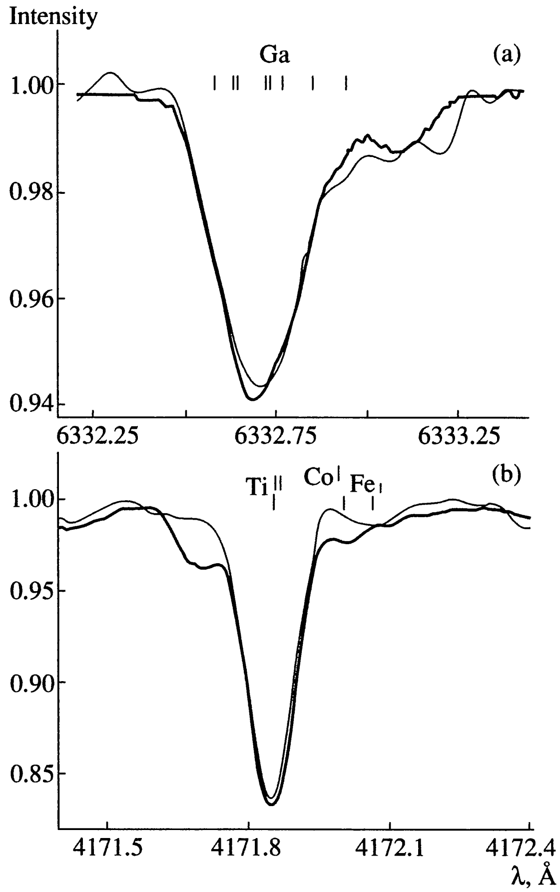

Fig. 5. (a) Spectrum of 46 Dra for component A near the GaII λ6678 Å line. The thin line is the observed spectrum, and the thick line is the synthetic spectrum. The wavelengths of the hyperfine-structure components (Lanz *et al.* 1993) are indicated by vertical bars. (b) The spectrum of 46 Dra near the GaII λ4172 Å line. The solid thick line denotes the synthetic spectrum for component B for log (Ga/H) = –6.98, the thin line is the observed profile, and the dot-dashed line is the synthetic spectrum for the solar Ga abundance. The wavelength scale in Figs. a and b is a laboratory scale.

$$M_B \sin^3 i = 0.07576 M_\odot,$$

$$M_A/M_B = 1.12.$$

Since the model atmospheres of the components of 46 Dra correspond, according to ARD, to main-sequence stars of luminosity class *V* with $T_{eff} = 11700$ and 11100 K, their masses can be estimated from the standard relations (Allen 1973): $4.80 M_\odot$ and $4.45 M_\odot$, which corresponds to $M_A/M_B = 1.079$, $\sin i = 0.5[(0.08482/4.8) + (0.7576/4.45)]^{1/3} = 0.256$, and the orbital inclination $i = 15°$.

The measured widths of the spectral lines in both components of 46 Dra are essentially identical and correspond to $V\sin i \leq 5$ km s^{-1} (the line width appears to be determined by the instrumental profile, because it is the same for stellar and atmospheric lines). Having estimated the standard radii of the components, $R_A = 3.2 R_\odot$ and $R_B = 3.0 R_\odot$ (Allen 1973), we can verify the assumption that the rotation of the components is synchronized with the orbital motion, and that their rotation axes are normal to the orbital plane. Assuming that $P_{rot} = P_{orb}$, we calculate the inclination of the rotation axis with respect to the line of sight using the relation

$$\sin i = P(V\sin i)_{obs}/2\pi R.$$

Substituting $P = 9^d.81073$, $R = 3.1 R_\odot$, and $(V\sin i)_{obs} \leq 5$ km s^{-1}, we obtain $i \leq 18°.4$, in good agreement with the above orbital inclination. Thus, the assumed atmospheric and orbital parameters agree with each other if the rotation and the orbital motion are synchronized.

Since our spectra covered a wide wavelength range, which was inaccessible in previous studies, we focused our attention on the careful identification of spectral lines and the measurement of their equivalent widths in order to obtain more reliable data (from a larger number of lines) or new data on the abundances of poorly studied chemical elements. We did not consider Zr and some iron-peak elements (Ti, Cr, Mn, Fe), whose abundances were accurately determined by ARD from a large number of lines.

We performed the line identification using the spectra obtained at all phases, which allowed us to exclude static atmospheric lines. The velocities of the components that were derived from the shift of lines are given in Table 2; they fall nicely on the radial-velocity curve of ARD.

The mean γ velocity as inferred from our spectra is –30.09 ± 0.43 km s^{-1}. The small number of points and the scatter of values make it impossible to confirm the assumption of ARD about the γ-velocity variations but are consistent with it.

The most complete separation of the lines of components A and B is observed at phase 0.067; we used the spectrum at this phase to measure the equivalent widths. We made our measurements using the DECH20 code. A comparison of our equivalent widths W_λ with the equivalent widths given in previous studies is given by the relations

$$W_\lambda(\text{Conti}) = 0.855 W_\lambda + 7.973,$$

$$W_\lambda(\text{Guthrie}) = 0.993 W_\lambda + 1.795,$$

$$W_\lambda(\text{ARD}) = 0.943 W_\lambda + 0.238.$$

The last relation is shown in Fig. 1. It has the smallest random scatter of values because of the good quality of the spectra in both studies.

5. DETERMINATION OF THE CHEMICAL COMPOSITION

To analyze the spectrum (identify the lines and determine the chemical composition), we used the BINARY code, which is designed to compute the synthetic spectrum of a SB2 star. This code was written by V.V. Tsymbal and is part of the STARSP software package that is based on the programs and data of Kurucz (1993). We determined the elemental abundances from the equivalent widths using the WIDTH9 code. Instead of the standard procedure of correcting the equivalent width of a line of one component for the effect of the spectrum of the other star, we directly calculated the equivalent width of the line in the composite spectrum using the formula

$$W_{A,B} = \int_{\lambda_0-\Delta\lambda}^{\lambda_0+\Delta\lambda} [(F_A L + SF_B L)/(F_A C + SF_B C)] d\lambda,$$

where F_AL, F_BL and F_AC, F_BC are the monochromatic fluxes in the line and in the continuum, respectively, computed for the adopted model atmospheres; and $S = (R_A/R_B)^2$. This approach automatically eliminates the need to seek a correction factor and allow for its wavelength dependence.

We computed all our model atmospheres using a modified ATLAS9 code and the OPDF tables of Kurucz (1993). An important feature of our computations was the selection of a criterion for the convergence of the model atmosphere. The point is that, by simply restricting the number of iterations to the achievement of a constant flux in each layer of the stellar atmosphere with an error of 1%, we run the risk of obtaining a significant error in the elemental abundances; this is especially true for strong lines. Therefore, we continued to compute the model until the temperature in each layer became constant, within a relative error of less than 1%.

As was pointed out above, an important point of our model-atmosphere calculations is allowance for chemical anomalies. In the case of 46 Dra, we must primarily allow for the He underabundance when calculating the model atmosphere of the star. Since allowance for the He underabundance has different effects on the Fe abundances determined from FeI and FeII lines (Fig. 2), disregarding the actual He abundance may result in an apparent break of the ionization equilibrium between FeI and FeII, which is commonly used for adjusting T_{eff}.

Our calculations for determining the He abundance from HeI profiles revealed some uncertainties which are associated with the theory of Stark broadening and with the programs of calculations we used. Figure 3 shows the computed profiles of the HeI λ4026 Å line for Kurucz's model with $T_{eff} = 15000$ K and $\log g = 4.0$ for the line broadening from Dmitrievic and Sahal-Breschot (1990) and for the broadening derived by Barnard *et al.* (1974) ("unified theory"). We used the unified theory in our calculations. Figure 4 compares the parts of the synthetic spectrum near two HeI lines that we calculated using our program. In general, our He abundances (see Table 3) lend support to the results of ARD.

We also used the method of synthetic spectrum to determine the Ga abundance from the Ga II λ6334 Å

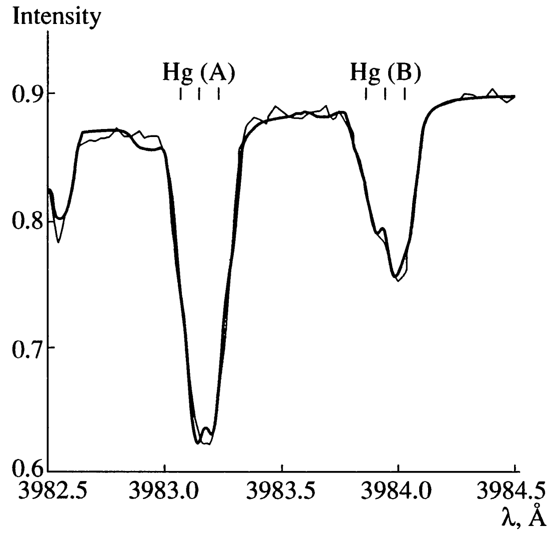

Fig. 6. The spectrum of 46 Dra near the HgII λ3984 Å line. The thin line is the observed spectrum, and the thick line is the synthetic spectrum. The wavelengths of ^{200}Hg, ^{202}Hg, and ^{204}Hg (Gouthrie 1984) are indicated by the vertical bars.

line (Fig.5), which has hyperfine structure (Lanz *et al.* 1993), and the isotopic composition of Hg from the HgII λ3984 Å line.

The synthetic spectra computed with allowance for the ^{200}Hg, ^{202}Hg, and ^{204}Hg isotopes [the wavelengths were taken from Guthrie (1984)] are shown in Fig. 6. Our calculations (Table 4) lend support to the significant difference in the isotopic composition of mercury in the atmospheres of the components of 46 Dra reported by Aikman and Cowley (1975).

In our abundance determinations, we used the following sources of atomic data: the lists of Luck (1977) and Kurucz (1988), the VALD database (Piskunov *et al.* 1995), and the lists of lines given for Hg–Mn stars by Adelman *et al.* (1994, 1995), ARD, and Roby and Lambert (1990).

Table 5 summarizes the results of our abundance determinations and compares them with those of ARD. In general, the results are in reasonably good agreement with each other, and the discrepancy reaches 0.3 dex very rarely.

The abundances determined from all lines of each element with measured equivalent widths and the atomic data used are given in Table 6.[1]

6. DISCUSSION OF THE RESULTS

Figure 7a clearly demonstrates the chemical anomalies in the components of 46 Dra. The abundance

[1] Table 6 is also published in electronic form and is accessible via ftp cdsarc.u-strasbg.fr/pub/cats/J (130.79.128.5) or http://cdsweb.u-strasbg.fr/pub/cats/J).

Table 5

	Component A		Component B	
ion	our data	ARD	our data	ARD
CI	-3.87 ± 0.26	–	-4.0 ± 0.13	–
CII	-3.56 ± 0.13	-3.94 ± 0.05	-3.83 ± 0.40	-3.94 ± 0.02
NI	-5.28 ± 0.18	–	-4.96 ± 0.18	–
OI	-3.47 ± 0.19	-3.73	-3.39 ± 0.24	–
NeI	-4.15 ± 0.22	–	-3.69 ± 0.18	–
NaI	-5.50 ± 0.08	–	-5.18 ± 0.11	–
MgI	-4.61 ± 0.24	-5.21 ± 0.18	-4.25 ± 0.25	-4.65 ± 0.58
MgII	-4.70 ± 0.16	-4.72 ± 0.19	-4.47 ± 0.29	-4.60 ± 0.24
AlI	–	-6.11 ± 0.15	-5.93	–
AlII	-6.56 ± 0.14	–	-5.65 ± 0.29	–
SiI	-4.74	-4.69	-4.75	–
SiII	-4.63 ± 0.18	-4.84 ± 0.18	-4.32 ± 0.14	-4.57 ± 0.29
SiIII	-4.33 ± 0.12	-4.33	–	–
PII	-5.19 ± 0.26	-5.13 ± 0.17	-5.49 ± 0.26	-5.57 ± 0.20
PIII	-5.09	–	–	–
SI	-4.72	–	–	–
SII	-4.99 ± 0.46	-4.97 ± 0.29	-4.59 ± 0.32	–
ClII	-6.16	–	–	–
ArI	$-5.02 \pm/-0.00$ (2)	–	$-5.03 \pm/-0.00$	–
ArII	-5.16	–	–	–
CaI	-5.56	–	-5.64	-5.49
CaII	-5.72 ± 0.23	-5.51	-5.68 ± 0.28	-5.57
ScII	-9.13 ± 0.32	-8.91	-9.29 ± 0.35	-9.71
VII	-7.76 ± 0.63	-7.95 ± 0.33	-7.51 ± 0.62	–
NiI	–	–	-5.45	–
NiII	-6.34 ± 0.44	–	-5.91 ± 0.52	–
GaI	-5.27	–	-6.86	–
GaII	-5.08 ± 0.22	-5.23 ± 0.10	–	–
SrII	-7.94 ± 0.09	-8.02 ± 0.15	-6.74 ± 0.10	-6.87 ± 0.15
YII	-7.76 ± 0.14	-7.93 ± 0.08	-7.69 ± 0.21	-7.80 ± 0.19
XeII	-5.83 ± 0.06	-5.70 ± 0.07	-5.59 ± 0.13	–
BaII	-8.97 ± 0.21	-9.07	-8.64 ± 0.90	–
PtII	-8.07 ± 0.26	-8.04 ± 0.34	-7.00 ± 0.16	-6.86 ± 0.47
AuII	-7.81 ± 0.15	-7.60 ± 0.07	-7.20 ± 0.11	-7.23 ± 0.00
HgI	-5.63	-5.98	-5.87	–
HgII	-5.22	-5.93	-5.16	–

Table 6. Elemental abundances in the photospheres of the components of 46 Dra Derived from individual lines of each ion. The first row gives the mean abundance for all lines of the ion

Species, λ Å	E_i (eV)	log*gf*	46 Dra A		46 Dra B	
			W((*m*Å)	logN/N_{tot}	*W*((*m*Å)	logN/N_{tot}
CI				–3.87 + 0.26		–4.00 + 0.13
4771.742	7.49	–1.700	1.5	–3.92	0.9	–4.06
4932.049	7.68	–1.879	1.3	–3.70		
7848.244	8.85	–0.919	1.3	–3.86	1.3	–3.79
9061.400	7.43	–0.280	18.2	–4.19	20.5	–4.01
9061.900	7.48	–0.030			29.0	–3.97
9062.500	7.48	–0.400			21.2	–3.85
9078.300	7.48	–0.450	12.7	–4.20	10.3	–4.25
9088.513	7.51	–0.510			14.7	–3.99
9094.800	7.49	0.120	71.1	–3.40	31.2	–4.10
9111.807	7.49	–0.470	24.6	–3.82	17.1	–3.96
CII				–3.56 + 0.13		–3.83 + 0.40
3918.968	16.33	–0.512	9.2	–3.60	1.6	–4.02
3920.681	16.33	–0.212	19.0	–3.35	7.8	–3.33
4267.001	18.05	0.609	15.3	–3.60	7.1	–3.48
4267.261	18.05	0.769	16.5	–3.69	5.3	–3.85
4737.966	13.72	–1.000			1.0	–4.47
NI				–5.28 + 0.18		–4.96 + 0.18
8188.300	10.33	–0.240			2.5	–4.73
8216.336	10.34	–0.009			2.3	–5.01
8629.200	10.69	0.090	1.4	–5.40	3.1	–4.89
8680.300	10.34	0.400			3.0	–5.06
8683.400	10.33	0.140	1.9	–5.29		
8686.200	10.33	–0.270	1.8	–4.98	2.6	–4.66
8703.300	10.33	–0.270			1.4	–5.16
8711.700	10.33	–0.160	1.3	–5.45	3.0	–4.94
8718.800	10.34	–0.230			1.3	–5.22
OI				–3.47 + 0.19		–3.39 + 0.24
4368.250	9.48	–1.650	4.0	–3.74	2.8	–3.74
4673.788	10.74	–2.219	1.6	–3.02		
5435.780	10.74	–1.646	1.1	–3.70		
6046.233	10.99	–1.889			1.2	–3.05
6155.976	10.74	–0.660	9.7	–3.62	6.7	–3.60
6156.766	10.74	–0.440	15.5	–3.59		
6158.184	10.74	–0.290	22.8	–3.51	13.2	–3.60
6453.602	10.74	–1.359	3.0	–3.45	3.2	–3.24
6454.445	10.74	–1.131	5.4	–3.40		
6455.976	10.74	–0.985			5.7	–3.33
7156.700	12.73	0.259	11.0	–3.40	9.7	–3.20
7886.270	14.37	0.237	1.8	–3.36		
8221.824	12.54	0.310	11.4	–3.41		

Table 6. (Contd.)

Species, λ Å	E_i (eV)	log*gf*	46 Dra A		46 Dra B	
			W((*m*Å)	logN/N_{tot}	*W*((*m*Å)	logN/N_{tot}
NeI				−4.15 + 0.22		−3.69 + 0.18
5852.488	16.85	−0.459	1.5	−4.17	1.0	−3.86
5881.895	16.62	−0.669	1.4	−4.09		
5944.834	16.62	−0.119			4.5	−3.39
5975.534	16.62	−1.009	1.1	−3.83		
6266.495	16.71	−0.529	1.2	−4.14		
6334.428	16.62	−0.309			1.3	−3.80
6402.246	16.62	0.360	3.3	−4.52		
7032.413	16.62	−0.249			1.1	−3.72
NaI				−5.50 + 0.		−5.18 + 0.11
5682.647	2.10	−0.710	1.0	−5.42	1.3	−5.22
5688.217	2.10	−0.400			1.9	−5.35
5889.973	0.00	0.110	31.1	−5.47	35.3	−5.09
5895.941	0.00	−0.190	16.1	−5.61	21.9	−5.27
8194.836	2.10	0.530			13.1	−5.12
4982.814	2.10	−0.949			1.3	−5.02
MgI				−4.61 + 0.24		−4.25 + 0.25
3829.355	2.71	−0.231	11.5	−4.79	15.1	−4.52
3832.304	2.71	0.121	11.8	−4.87	19.4	−4.06
3838.292	2.72	0.392			14.1	−3.65
4167.271	4.35	−1.004	1.0	−4.54	2.9	−4.17
4702.991	4.35	−0.666	4.3	−4.23	4.6	−4.30
5167.322	2.71	−1.029	11.2	−4.21	10.1	−4.35
5172.684	2.71	−0.399	13.0	−4.76	20.0	−4.47
5183.604	2.72	−0.179	19.2	−4.74	25.9	−4.40
5528.405	4.35	−0.619	1.6	−4.72	4.3	−4.36
MgII				−4.70 + 0.16		−4.47 + 0.29
3848.211	8.86	−1.590	10.7	−4.65	5.5	−4.68
3850.386	8.86	−1.840	9.1	−4.53	8.4	−4.24
4384.637	10.00	−0.790	15.5	−4.86	14.9	−4.57
4390.572	10.00	−0.530	24.8	−4.83	19.6	−4.64
4427.994	10.00	−1.210	8.9	−4.72	7.2	−4.56
4433.988	10.00	−0.910	19.3	−4.58	11.3	−4.59
4481.126	8.86	0.740	114.1	−4.41	84.6	−3.76
4481.325	8.86	0.590	100.7	−4.52	72.0	−4.14
4739.593	11.57	−0.660	3.4	−5.01	2.6	−4.87
7877.059	9.99	0.390	47.9	−4.76	29.9	−4.66
7896.378	10.00	0.648	58.1	−4.73	41.3	−4.36
8234.636	10.00	0.030	31.8	−4.76		
8213.987	10.00	−0.269			16.3	−4.54
AlI				−5.93 + 0.00		
3944.006	0.00	−0.623			6.9	−5.93

Table 6. (Contd.)

Species, λ Å	E_i (eV)	log*gf*	46 Dra A		46 Dra B	
			W((*m*Å)	logN/N_{tot}	*W*((*m*Å)	logN/N_{tot}
AlII				–6.70 + 0.23		–5.65 + 0.29
5593.228	13.26	0.410			2.2	–5.77
7042.048	11.32	0.350	1.8	–6.84	5.2	–5.82
7056.612	11.32	0.130	1.0	–6.89	3.3	–5.86
7063.642	11.32	–0.349	1.1	–6.37	5.0	–5.14
SiI				–4.74 + 0.00		–4.75 + 0.00
3905.532	1.91	–0.757	15.2	–4.74	12.8	–4.75
SiII				–4.63 + 0.18		–4.32 + 0.14
3853.665	6.86	–1.517	41.3	–4.55	29.6	–4.18
3856.018	6.86	–0.557	68.9	–4.77	45.1	–4.52
3862.595	6.86	–0.817	62.1	–4.70	49.7	–4.14
4075.452	9.84	–1.403	11.5	–4.52	8.3	–4.27
4076.780	9.84	–1.668	9.2	–4.39	7.5	–4.07
4128.054	9.84	0.316	77.8	–4.33	51.5	–4.01
4130.894	9.84	0.476	68.0	–4.70	45.1	–4.41
4190.707	13.49	0.000	5.8	–4.82	5.8	–4.41
4198.134	13.49	–0.300	4.5	–4.66	4.3	–4.29
4200.657	12.52	–0.819	1.8	–4.97		
4200.898	12.53	–0.670	5.2	–4.64	4.8	–4.32
4621.418	12.53	–0.540			3.7	–4.45
4621.722	12.53	–0.380	5.9	–4.77	4.4	–4.53
4673.256	12.84	–0.600	4.2	–4.56	2.6	–4.40
5041.030	10.07	0.174	48.7	–4.66	31.4	–4.44
5055.980	10.07	0.441	54.4	–4.79	37.3	–4.46
5056.314	10.07	–0.530	26.2	–4.57	19.7	–4.23
5185.555	12.84	–0.389	3.3	–4.77	3.8	–4.30
5957.560	10.07	–0.350	27.7	–4.55	18.8	–4.28
5978.930	10.07	–0.061	37.6	–4.55	23.9	–4.32
6371.355	8.12	–0.050	72.3	–4.60	50.0	–4.19
6829.799	12.88	–0.269	4.5	–4.10		
7848.800	12.53	0.335	5.4	–4.83	4.7	–4.39
7849.720	12.53	0.492	7.6	–4.80	4.8	–4.53
SiIII				–4.33 + 0.12		
4552.622	19.02	0.181	2.0	–4.45		
4567.840	19.02	–0.039	2.0	–4.21		
PII				–5.19 + 0.26		–5.49 + 0.23
4019.509	9.518	–1.908	2.4	–5.03		
4044.576	13.311	0.481	10.7	–5.03	3.8	–5.20
4064.727	12.813	–0.714	0.9	–5.36		
4224.522	13.311	0.496			0.9	–5.94
4230.220	13.311	–1.260	1.5	–4.36		
4414.292	13.056	–0.560	1.0	–5.29		
4420.712	11.021	–0.478	9.1	–4.98	2.9	–5.20

Table 6. (Contd.)

Species, λ Å	E_i (eV)	log*gf*	46 Dra A		46 Dra B	
			W((*m*Å)	log*N*/N_{tot}	*W*((*m*Å)	log*N*/N_{tot}
4424.091	13.056	–0.816	1.6	–4.83		
4463.027	13.087	0.026	4.8	–5.13		
4466.140	13.087	–0.283	1.1	–5.51		
4475.270	13.087	0.301	9.2	–5.07	2.4	–5.31
4483.693	13.056	–0.431	1.9	–5.12		
4499.230	13.381	0.377	6.1	–5.12	0.9	–5.69
4530.823	13.056	–0.020	4.3	–5.13	1.3	–5.28
4558.095	13.143	–0.056	2.6	–5.25		
4565.287	13.143	–0.243	1.4	–5.39		
4588.032	12.813	0.575	10.3	–5.32		
4602.069	12.853	0.799	13.8	–5.34	3.1	–5.72
4626.708	12.813	–0.203	3.7	–5.08		
4658.309	12.853	–0.412	2.1	–5.12		
4679.028	13.143	–0.404	1.7	–5.07		
4935.626	13.825	–0.039	1.4	–5.17		
4954.355	12.790	–0.369	1.3	–5.31		
5253.517	11.021	0.280	21.3	–4.82		
5296.093	10.802	0.050	11.3	–5.22		
5344.709	10.736	–0.279	7.7	–5.27		
5386.872	10.754	–0.179	7.8	–5.34		
5409.713	10.754	–0.249	9.5	–5.15		
5425.885	10.802	0.370	19.0	–5.29	3.8	–5.78
5450.706	13.086	–0.049	1.6	–5.26		
5461.172	13.961	0.470	1.0	–5.62		
6034.035	10.736	–0.139	9.7	–5.06	2.5	–5.33
6043.055	10.802	0.400	19.5	–5.08	4.1	–5.57
6087.829	10.754	–0.309			1.5	–5.40
6165.571	10.802	–0.399	4.5	–5.19	0.9	–5.51
6459.941	10.934	0.560	11.1	–5.42	4.4	–5.45
6503.406	10.906	0.620	7.4	–5.74		
6508.038	10.886	0.620	6.1	–5.86		
7845.601	11.021	–0.039	6.5	–4.88		
PIII				–5.09 + 0.00		
4059.312	14.492	–0.080	2.0	–5.09		
SI				–4.72 + 0.00		
6757.195	7.870	–0.290	1.0	–4.72		
SII				–5.14 + 0.37		–4.59 + 0.32
3923.445	16.198	0.440	1.6	–5.14	1.6	–4.87
4028.778	15.943	–0.119	2.6	–4.68		
4142.259	15.848	0.240			2.0	–4.59
4145.060	15.867	0.230	1.9	–5.16	2.0	–4.58
4146.912	17.386	0.660			1.1	–4.80
4153.068	15.899	0.395	2.6	–5.14		

Table 6. (Contd.)

Species, λ Å	E_i (eV)	log*gf*	46 Dra A		46 Dra B	
			W((*m*Å)	logN/N_{tot}	*W*((*m*Å)	logN/N_{tot}
4162.665	15.944	0.830	2.0	−5.71	2.3	−5.08
4162.693	15.943	0.830			5.2	−4.49
4168.410	15.866	−0.159	0.8	−5.21		
4189.613	17.396	0.190	1.9	−4.57		
4217.225	15.943	−0.149	1.1	−5.02		
4249.913	17.445	−0.009	1.2	−4.56		
4267.762	16.100	0.256			1.8	−4.55
4278.528	16.091	−0.109	2.0	−4.66		
4294.402	16.135	0.549			1.6	−4.85
4391.822	15.898	−0.559	1.0	−4.57		
4463.599	15.943	0.130			2.4	−4.20
4483.439	15.898	−0.319	1.2	−4.70	1.6	−4.02
4524.675	15.068	0.076			2.0	−4.58
4552.373	15.067	−0.099			2.7	−4.20
4716.271	13.617	−0.319	1.0	−5.56	3.6	−4.31
4819.596	16.197	−0.219			1.0	−4.08
4917.982	13.676	−0.739			2.2	−4.06
4925.323	13.583	−0.229			1.7	−4.77
4942.456	13.583	−0.589	1.0	−5.21	2.9	−4.09
5013.999	14.066	0.030			2.5	−4.57
5027.185	13.092	−0.459	1.1	−5.47	1.9	−4.66
5032.386	13.671	0.280	1.9	−5.70	2.0	−5.13
5212.229	15.067	0.660			1.3	−5.10
5212.579	15.067	0.660	3.8	−5.05	3.1	−4.57
5320.695	15.067	0.540	0.9	−5.67	3.5	−4.32
5432.744	13.617	0.310			1.6	−5.15
5526.188	13.701	−0.479	1.6	−4.84		
5606.088	13.733	0.160	1.7	−5.41	2.3	−4.67
5616.614	13.659	−0.469			1.5	−4.32
5639.980	14.067	0.330	2.0	−5.34	2.0	−4.77
5640.314	13.701	0.150	1.9	−5.34	2.2	−4.69
5646.979	14.002	0.110			1.1	−4.91
5664.760	13.659	−0.299	0.9	−5.27	1.0	−4.69
ClII				−6.16 + 0.00		
4794.556	13.375	0.460	1.1	−6.16		
ArI				−5.02 + 0.00		−5.03 + 0.00
7514.651	11.623	−0.439			1.0	−5.03
8264.522	11.827	−0.289	1.5	−5.02		
ArII			−5.16			
4426.004	16.748	0.240	1.0	−5.16		
CaI			−5.56			−5.64
+0.00						
4426.728	0.000	0.243	2.2	−5.56	3.8	−5.64

Table 6. (Contd.)

Species, λ Å	E_i (eV)	log*gf*	46 Dra A		46 Dra B	
			W((*m*Å)	logN/N_{tot}	*W*((*m*Å)	logN/N_{tot}
CaII				−5.72 + 0.23		−5.68 + 0.28
3933.663	0.000	0.134	142.6	−5.49	107.9	−5.31
4220.071	7.514	−1.329	1.3	−5.39		
5339.217	8.440	−0.050			6.1	−5.28
8248.802	7.510	0.570	10.4	−5.98	9.4	−5.93
8254.681	7.500	−0.380			2.6	−5.68
8912.068	7.047	0.640	30.2	−5.89	21.4	−5.96
8927.356	7.049	0.790	39.5	−5.83	27.6	−5.90
ScII				−9.31 + 0.20		−9.37 + 0.35
4246.822	0.315	0.320	3.2	−9.55	2.0	−9.86
4320.732	0.605	−0.260	0.8	−9.44		
4374.457	0.618	−0.440	0.9	−9.22		
4400.389	0.605	−0.513	1.2	−9.03		
4415.545	0.595	−0.639			1.0	−9.07
5526.790	1.768	0.130			1.1	−9.18
VII				−8.38 + 0.14		−7.67 + 0.39
4002.936	1.428	−1.472			1.2	−7.74
4005.706	1.817	−0.460	1.5	−8.52	1.7	−8.39
4008.170	1.793	−1.773			1.0	−7.33
4023.388	1.805	−0.518			1.8	−8.31
4035.627	1.793	−0.622	2.0	−8.24	3.5	−7.89
4036.782	1.476	−1.540			1.9	−7.44
4065.071	3.796	−0.238			2.1	−7.48
4225.222	2.026	−1.160			1.8	−7.56
4232.044	3.973	−0.587			1.0	−7.40
4532.172	3.799	−0.756			1.4	−7.16
NiI						−5.45 + 0.00
4401.540	3.193	0.080			1.2	−5.45
NiII				−6.34 + 0.44		−5.91 + 0.52
4067.031	4.029	−1.835	1.8	−7.05	2.8	−6.56
4187.849	4.029	−2.659			6.4	−5.28
4679.159	6.989	−1.748	1.4	−5.85		
4992.023	12.252	1.100	1.6	−6.26	1.6	−5.88
4362.099	4.029	−2.709	1.5	−6.20		
GaI				−5.27 + 0.00		−7.00 + 0.00
4172.039	0.102	−0.270	25.4	−5.27	synth	−7.00
GaII				−5.11 + 0.22		
4251.149	14.112	0.350	17.3	−4.82		
4254.075	14.115	−0.230	7.2	−5.04		
4255.722	14.115	0.680	22.8	−4.83		
5338.270	14.680	−0.210	1.8	−5.33		
5421.310	14.720	−0.140	1.7	−5.39		
6334.050	12.760	0.360	synth	−5.25		

Table 6. (Contd.)

Species, λ Å	E_i (eV)	log*gf*	46 Dra A		46 Dra B	
			W((*m*Å)	log*N*/N_{tot}	*W*((*m*Å)	log*N*/N_{tot}
SrII				–7.94 + 0.09		–6.74 + 0.10
4077.709	0.000	0.167	28.7	–7.93	32.3	–6.77
4161.792	2.940	–0.502	1.9	–7.81		
4215.519	0.000	–0.145	23.9	–7.97	30.9	–6.61
4305.443	3.040	–0.136	2.1	–8.07	12.9	–6.85
YII				–7.76 + 0.14		–7.69 + 0.21
3930.660	0.409	–1.610			3.0	–7.40
3950.352	0.104	–0.490	12.9	–7.75	12.7	–7.60
3982.594	0.130	–0.490	10.9	–7.80	8.6	–7.89
4177.529	0.409	–0.160	19.5	–7.60	14.0	–7.71
4235.729	0.130	–1.500	1.7	–7.85	5.9	–7.31
4309.631	0.180	–0.750	4.8	–8.07	6.4	–7.96
4358.728	0.104	–1.320	2.5	–7.83	5.6	–7.48
4374.935	0.409	0.160	19.1	–7.93	17.0	–7.68
4398.013	0.130	–1.000	4.3	–7.91	3.4	–8.12
4422.591	0.104	–1.270	3.0	–7.83	4.7	–7.69
4682.324	0.409	–1.510	1.3	–7.83	1.1	–8.03
4786.578	1.032	–1.292	2.3	–7.48	2.0	–7.63
4883.685	1.083	–0.041	14.8	–7.63	14.2	–7.52
4900.110	1.032	–0.090	12.8	–7.74	12.0	–7.74
5205.731	1.033	–0.342	10.2	–7.65		
5662.930	1.944	0.200	10.7	–7.68	10.7	–7.65
6613.735	1.740	–1.097	1.1	–7.60	1.2	–7.66
7881.881	1.830	–0.602	2.0	–7.74		
XeII				–5.83 + 0.06		–5.59 + 0.13
4180.100	13.860	0.170	1.8	–5.86		
4245.380	13.890	0.420	2.6	–5.88	2.4	–5.45
4603.040	11.790	–0.080	4.9	–5.74	2.2	–5.72
BaII				–8.99 + 0.19		–8.78 + 0.12
4554.029	0.000	0.170	4.3	–9.03	5.3	–8.93
4934.095	0.000	–0.155	1.3	–9.28		
6141.713	0.704	–0.080	1.6	–8.87	3.0	–8.64
6496.897	0.604	–0.380	1.1	–8.78	1.4	–8.76
PtII				–8.07 + 0.26		–7.00 + 0.16
4034.170	4.000	–0.840	1.1	–8.36	5.1	–7.27
4046.450	4.520	0.000	8.1	–7.93	15.6	–6.92
4061.660	3.630	–0.720	7.0	–7.71	12.2	–6.86
4514.170	3.630	–0.480	3.8	–8.27	14.4	–6.93
UII				–7.51 + 0.46		–7.20 + 0.11
4016.070	6.015	–1.000	1.8	–7.97	3.4	–7.31
4052.790	6.015	–1.000	9.7	–7.04	4.9	–7.09
HgI				–5.63 + 0.00		–5.78 + 0.00
4358.343	4.870	–0.450	5.9	–5.63	3.9	–5.78
HgII				–5.74 + 0.09		–5.79 + 0.21
3983.960	4.400	–1.730	synth	–5.78	synth	–6.06
6149.475	11.870	0.328	5.5	–5.83	3.5	–5.58

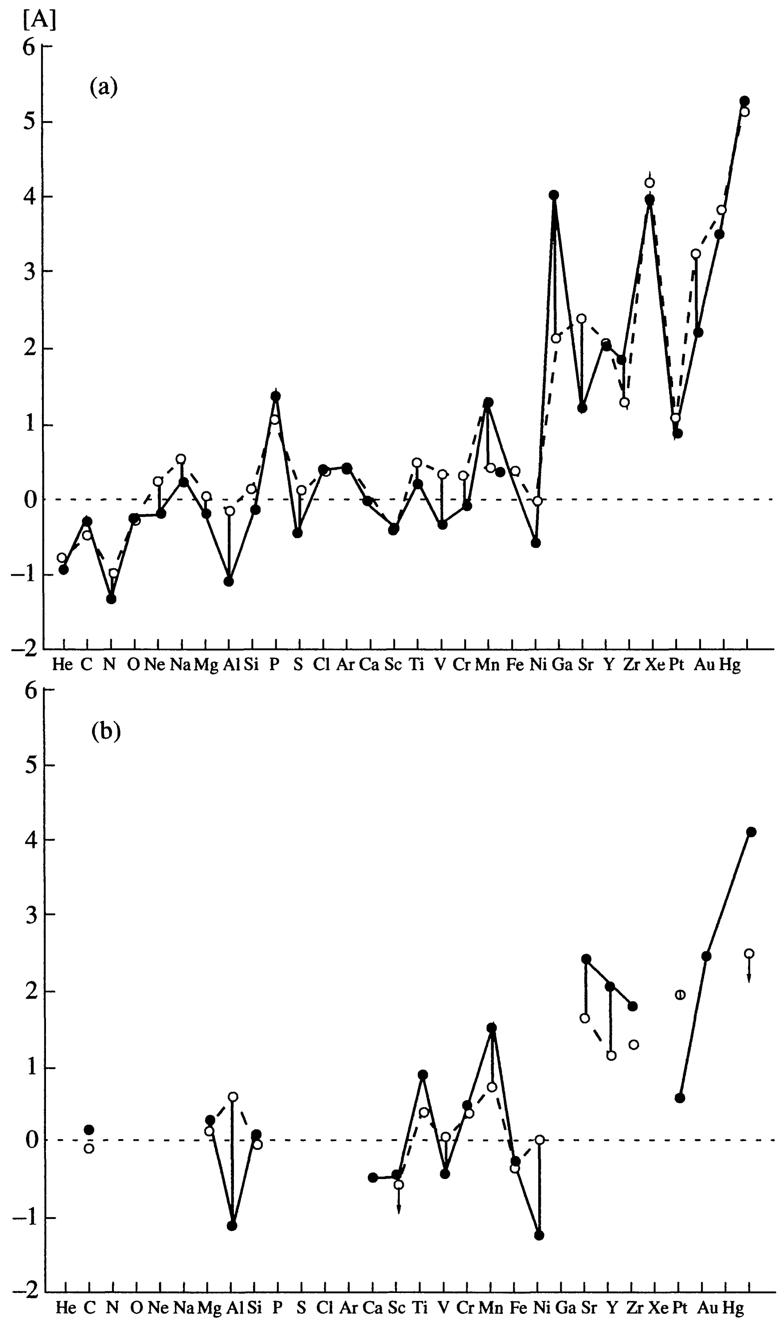

Fig. 7. (a) Elemental abundances in the atmospheres of 46 Dra A (filled circles) and 46 Dra B (open circles) relative to the Sun on a logarithmic scale. For Cr, Mn, and Fe, we used the values from Adelman *et al.* (1997). (b) The same as in Fig. (a) for AR Aur A and *B* (Khokhlova *et al.* 1995).

curves for both components are almost identical except for the small differences for Ne, Al, S, V, Ni, and Zr and the significant differences for Mn, Ga, Sr, and Pt. In addition, there is a considerable difference between the components of 46 Dra in the isotopic composition of mercury: according to our calculations, ^{202}Hg is the main (85%) isotope in the atmosphere of the primary, while the atmosphere of the secondary is dominated by the heaviest stable isotope ^{204}Hg, which accounts for 81% of the total Hg abundance.

Of interest is to compare our results with the peculiarities of the chemical composition of the components of the SB2 system AR Aur (Fig. 7b), which is similar in its properties to 46 Dra (Khokhlova *et al.* 1995). Unfortunately, because of the great line widths in the spectrum of AR Aur ($V\sin i = 23$ km s^{-1}), and because of the limited wavelength coverage, the number of unblended lines that were suitable for analysis and the number of studied elements were considerably smaller than those for 46 Dra. Both systems have components of approximately equal mass of a spectral type near B9 V and rotation synchronized with the orbital motion. The components of these systems are undoubtedly main-sequence stars, although their age within the main sequence is not known. The suggestion about extreme youth of AR Aur made by Nordstrom and Johansen (1994) is the result of a misunderstanding: judging by its distance, the star cannot be a member of the OB association; in addition, $\log g = 4.3$ determined from eclipse data is 0.6 dex greater than the effective gravity $\log g_{\rm eff} = 3.7$ derived from Balmer-line profiles by Tsymbal. This value is most likely overestimated.

It is natural to assume that 46 Dra and AR Aur are similar in evolutionary history. Figures 7a and 7b show that the abundance curves for components A and B of 46 Dra are very similar, while in the case of AR Aur, they differ much more greatly. In both cases, the same elements exhibit "peculiar" behavior: the difference of the Al and Ni underabundances and of the Mn, Sr, and Y overabundances in components A and B of both systems is undoubtedly significant. The heaviest elements show the greatest difference between the systems: Ba, Pt, and Hg behave differently in 46 Dra and AR Aur.

The general similarity of the abundance curves for components A and B may be a result of a common formation mechanism for anomalies, which is natural for stars that are born together and with such similar physical parameters; it does not rule out the possibility that the anomalies are formed in the protostellar cloud. However, whereas anomalies affect only the upper layer of a star, the observed differences in the chemical composition of the atmospheres of the components could arise only after the synchronization of the rotation and the orbital motion, i.e., after the termination of intense mixing.

A detailed study of other similar SB2 systems may help clarify the question of when the anomalies were formed. Our study at least suggests that the differences in the anomalies of the components of 46 Dra could arise during or after their arrival at the main sequence but in any case after the synchronization of the rotation with the orbital motion.

ACKNOWLEDGMENTS

We are grateful to Vincent Woolff (University of Texas) for great assistance in the preliminary reduction of the spectra. We also wish to thank the authors of ARD's study (in particular, T.A. Ryabchikova) for allowing us to use their results on 46 Dra prior to publication. This work was supported in part by the program "Astronomy" (project no. 3-292), by the US National Science Foundation (grant no. AST-9618414), and by the Robert A. Welch Foundation of Houston, Texas.

REFERENCES

Adelman, S.J., *Mon. Not. R. Astron. Soc.*, 1994, vol. 266, p. 97.

Adelman, S.J., *Mon. Not. R. Astron. Soc.*, 1995, vol. 280, p. 130.

Adelman, S.J., Ryabchikova, T.A., and Davidova, E.S., *Mon. Not. R. Astron. Soc.*, 1997 (in press).

Adelman, S.J. and Pyper, D.M., *Astron. J.*, 1979, vol. 84, p. 1603.

Aikman, G.C.L., *Publ. Dominion. Astrophys. Obs.*, 1976, vol. 14, p. 379.

Aikman, G.C.L. and Cowley, Ch.R., *Publ. Astron. Soc. Pac.*, 1975, vol. 87, p. 513.

Allen, C.W., *Astrophysical Quantities*. Translated under the title *Astrofizicheskie velichiny*, Moscow: Mir, 1973.

Auer, L.H., Mihalas, D., Aller, L.H., and Ross, J.E., *Astrophys. J.*, 1966, vol. 145, p. 153.

Barnard, A.J., Cooper, J., and Smith, E.W., *J. Quant. Spectrosc. Radiat. Transfer*, 1974, vol. 14, p. 1025.

Batten, A., *Doudle and Multiple Stars*. Translated under the title *Dvoinye i kratnye zvezdy*, Moscow: Mir, 1976.

Galazutdinov, G., *Spec. Astrophys Obs. Preprint Ser.*, Russ. Akad. Nauk, 1994.

Guthrie, B.N.G., *Mon. Not. R. Astron. Soc.*, 1984, vol. 206, p. 85.

Dmitrievic, M.S. and Saha-Breschot, S., *Astron. Astrophys., Suppl. Ser.*, 1990, vol. 82, p. 519.

Conti, P.S., *Astron. Astrophys.*, 1970a, vol. 7, p. 213.

Conti, P.S., *Astrophys. J.*, 1970b, vol. 160, p. 1077.

Kurucz, R.L., *Tape List*, Smithsonian Astrophys. Obs., 1988.

Kurucz, R.L., *CD-ROMs*, Smithsonian Astrophys. Obs., 1993.

Luck, R.E., *Astrophys. J.*, 1977, vol. 218, p. 752.

Lanz, T., Artru, M.C., Didelon, P., and Mathys, G., *Astron. Astrophys.*, 1993, vol. 272, p. 465.

Leone, F. and Manfre, M., *Astron. Astrophys.*, 1997, vol. 320, p. 257.

Nordstrom, B. and Johansen, K.T., *Astron. Astrophys.*, 1994, vol. 282, p. 787.

Petrie, R.M., *Publ. Dominion. Astrophys. Obs.*, 1935, vol. 6, p. 285.

Piskunov, N.E., Kupka F., Ryabchikova T.A., *et al.*, *Astron. Astrophys., Suppl. Ser.*, 1995, vol. 112, p. 525.

Roby, S.W. and Lambert, D.L., *Astrophys. J., Suppl. Ser.*, 1990, vol. 73, p. 67.

Sadakane, K., Takada, M., and Jugaku, K., *Astrophys. J.*, 1983, vol. 274, p. 261.

Takada-Hidai, M., Sadakane, K., and Jugaku, K., *Astrophys. J.*, 1986, vol. 304, p. 425.

Tull, R.G., McQueen, P.J., Sneden, Ch., and Lambert, D.L., *Publ. Astron. Soc. Pac.*, 1995, vol. 107, p. 251.

Khokhlova, V.L., Zverko, Yu., Zhizhnovskii, I., and Griffin, R.E.M., *Pis'ma Astron Zh.*, 1995, vol. 21, p. 908.

Khokhlova, V.L.,Vasil'chenko, D.V., and Stepanov, V.V., *Pis'ma Astron. Zh.*, 1997, vol. 23, p. 532.

Tsymbal, V.V., *Model Atmospheres and Stellar Spectra*, ASP Conf. Ser., Adelman, S.J. and Weiss, W.W., Eds., 1996, vol. 108, p. 198.

Translated by V. Khokhlova